RSC Sustainability

ROYAL SOCIETY OF CHEMISTRY

PERSPECTIVE

View Article Online
View Journal | View Issue

Cite this: *RSC Sustainability*, 2024, **2**, 3769

Green gold: prospects of lignin in organic electronics and bioelectronics

Laura Tronci[a] and Assunta Marrocchi *[b]

Lignin, a complex aromatic polymer from plant cell walls, has emerged as a promising material for organic electronics and bioelectronics due to its abundance, low cost, and renewability. Its unique chemical structure allows for the development of flexible, lightweight devices in organic electronics, from printed circuit boards, batteries and supercapacitors to field-effect transistors and solar cells, while its biocompatibility and low toxicity make it ideal for bioelectronic applications like in biosensors, artificial neural networks and cognitive computing. This perspective highlights lignin's potential to address sustainability challenges in the electronics industry and explores its current advancements and future prospects in these fields.

Received 7th August 2024
Accepted 27th October 2024

DOI: 10.1039/d4su00452c

rsc.li/rscsus

Sustainability spotlight

Lignin, a naturally occurring biopolymer, has rapidly emerged as a cornerstone in the development of sustainable and high-performance organic (bio)electronics. In organic electronics, lignin's role extends beyond simple substitution of materials. Its inherent properties can be leveraged to design devices with enhanced performance and functionality. It can be processed into flexible, lightweight, and cost-effective printed circuit boards, providing a sustainable alternative to rigid, resource-intensive traditional boards. Additionally, lignin-based organic field-effect transistors hold promise for creating high-performance, low-cost electronic devices with a reduced environmental impact. Moreover, lignin-based materials exhibit promising potential in energy storage solutions, such as batteries and supercapacitors, offering increased efficiency and longevity. Furthermore, lignin's versatility includes energy generation through its use in developing efficient solar cells. The intersection of lignin and organic bioelectronics is particularly promising. Lignin's biocompatibility allows for seamless integration with biological systems, enabling the development of advanced devices like biosensors and neural interfaces. This Perspective highlights recent advancements in these key areas, underscoring lignin's evolution from a promising material to a versatile platform for sustainable electronic innovations. By identifying key opportunities and challenges, this analysis aims to serve as a catalyst for fostering collaboration and investment in lignin-based technologies. This work aligns with the United Nations' Sustainable Development Goals (SDGs) 7 (Affordable and Clean Energy), 9 (Industry, Innovation, and Infrastructure), 12 (Responsible Consumption and Production), and 13 (Climate Action), addressing critical sustainability challenges by promoting the use of renewable materials, reducing electronic waste, and contributing to cleaner energy solutions.

Introduction

Lignin, a complex aromatic polymer found in the cell walls of plants, is traditionally recognized for its role in providing overall stiffness and resistance to microbial attack.[1]

Recently, its potential has extended to the burgeoning fields of organic (bio)electronics, driven by the electronics industry's search for sustainable and efficient alternatives amid significant environmental and economic challenges. The push for biodegradable and renewable materials in electronic devices positions lignin as a promising candidate due to its abundance, low cost, and renewability—key attributes essential for a green electronics industry capable of meeting growing market demands.[2,3]

Incorporating lignin into electronic devices offers the dual benefits of mitigating environmental pollution and addressing hazardous disposal practices that pose serious health risks. Moreover, leveraging renewable resources like lignin can help prevent crises similar to the semiconductor shortage of 2020,[4] which was exacerbated by the covid-19 pandemic, geopolitical tensions, and environmental factors.

Lignin's unique chemical composition, featuring a network of various structures and functional groups, opens up numerous possibilities for its application in electronics, particularly in organic electronics and bioelectronic devices. This composition allows the isolation of several building block molecules whose properties often surpass those of petroleum-derived molecules, polymers, and minerals currently used in these technologies.

These lignin-derived molecules are particularly beneficial in organic electronics, which utilize organic materials to construct flexible, lightweight, and potentially lower-cost devices such as smartphones, smartwatches, tablets, [5,6] sensors, solar cells, and light emitting diodes.[7]

[a]*Soc. Agr. Iraci Borgia s.s., Via Cantone 5, Bevagna (PG), Italy. E-mail: troncilaura4@gmail.com*

[b]*Department of Chemistry, Biology and Biotechnology, University of Perugia, Via Elce di Sotto 8, Perugia 06123, Italy. E-mail: assunta.marrocchi@unipg.it*

Similarly, bioelectronics, which interface electronic devices with biological systems,[5] benefit from lignin's inherent biocompatibility and low toxicity, making them suitable for biosensors and medical implants. These applications take advantage of lignin's renewable nature and seamless integration with biological tissues, promising advancements in medical technology and diagnostics.

This perspective aims to highlight the transformative role of lignin and its derivatives in the electronics industry, particularly within organic electronics and bioelectronics technologies. Existing reviews[7–12] have addressed only specific aspects of lignin's application in this context. In contrast, this perspective offers a comprehensive examination of lignin's structural characteristics and its diverse applications across key areas of the organic (bio)electronics industry. We begin with an essential overview of lignin's structural properties to lay the groundwork for understanding its potential in electronics. Following this, we delve into each application area, discussing successful research studies and comparing various approaches.

Laura Tronci

Laura Tronci holds a degree in Molecular and Industrial Biotechnology from the University of Perugia. Since 2021, she has been working as a plant operator at a biogas facility located in Bevagna, in the province of Perugia. In this role, she oversees the operation and optimization of the biogas plant, ensuring efficient energy production while adhering to environmental and safety standards. Her academic background and professional experience have allowed her to develop strong expertise in renewable energy and sustainability practices.

Assunta Marrocchi

Assunta Marrocchi is an Associate Professor of Organic Chemistry at the University of Perugia (Italy), Department of Chemistry, Biology and Biotechnology. Following her PhD in Chemical Sciences at the same Institution, she held postdoctoral and academic research positions, and she joined Radboud University Nijmegen (The Netherlands) and Northwestern University (IL, USA) as a visiting scientist. Her education and professional career are primarily centered on organic synthesis-themed research, with a focus on advanced organic materials and their application in organic electronics, and sustainable conversion of biomass into high added value chemicals, fuels, and materials.

This holistic view not only showcases the current advancements in lignin-based organic (bio)electronics but also aims to provide points of reflection on future possibilities for integrating lignocellulosic biomass into the large-scale electronics industry.

Lignin: source, structural characteristics and properties

Lignocellulosic biomass, the most abundant renewable material on earth, is the primary natural source of lignin. As illustrated in Fig. 1, lignin forms an integral component of plant cell walls, where it is chemically interwoven with hemicellulose and wrapped around cellulose fibres in plant cell walls, where it serves as a critical binder between these two polysaccharides. This complex structure provides mechanical strength to herbs, plants, and large trees. Additionally, lignin regulates water transport, protects against biological stresses by inhibiting enzymatic degradation of other components, and acts as an antibacterial agent against microorganisms.[13] Lignin consists of a highly heterogeneous collection of phenolic compounds, forming an amorphous, hydrophobic, and cross-linked macromolecular structure. The building blocks of this network are three basic monolignol subunits with varying degrees of methoxylation: synapyl alcohol, coniferyl alcohol, and *p*-coumaryl alcohol. These subunits link together to form syringyl (S), guaiacyl (G), and *p*-hydroxyphenyl (H) groups (Fig. 1).[14] The proportion of these monomers in any given lignin sample is indicative of its source, making the measurement of H/G/S ratios analytically important. For instance, hardwood lignin (*e.g.*, eucalyptus, poplar, birch) primarily consists of G and S with small quantities of H subunits, while softwood lignin (*e.g.*, spruce, pine) is mainly composed of G units with small quantities of H. [15] In herbaceous plants, the three monolignols are present in almost equal proportions, resulting in H-G-S type lignin. Other less abundant monomers identified in lignin include acylated monolignols like acetates, *p*-coumarates, and *p*-hydroxybenzoates, as well as compounds with a 5-hydroxyguaiacyl structure, such as 3-methoxycatechol, 5-vinyl-3-methoxycatechol, and 5-propenyl-3-methoxycatechol.[16] During lignin biosynthesis, monolignols undergo *in situ* radical polymerization, generating interunit linkages such as aryl ether (α-O-4′ and β-O-4′), resinol

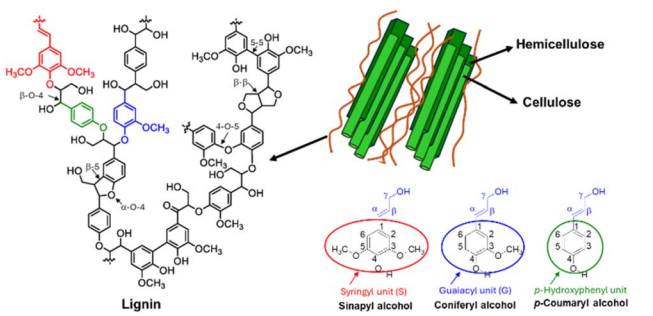

Fig. 1 Schematic representations of structure and positioning of lignin in lignocellulosic biomass.

(β-β′), phenylcoumaran (β-5′), biphenyl (5–5′), and 1,2-diaryl propane (β-1′) – Fig. 1.

At the industrial level, lignin is extracted through chemical pulping processes, which affect its chemical functional groups and properties. Generally, there are two strategies for separating lignin from its source: (i) selective hydrolysis of polysaccharides, leaving lignin in the solid residues, and (ii) degradation of lignin into soluble fragments, followed by removal of the solid residue and extraction of lignin using an appropriate solvent. Most industrial pulping processes belong to the second method, which includes sulfur processes (producing lignosulfonate and kraft lignin) and sulfur-free processes (producing organosolv lignin and soda lignin). In sulfur processes, sulfur acts as a catalyst, resulting in functional groups containing sulfur remaining bound to the lignin. In contrast, sulfur-free processes do not involve sulfur, resulting in lignin without sulfur-containing functional groups. The extraction method significantly affects the reactivity of the extracted lignin.

The kraft pulping process is the most established industrial method, used primarily in the paper industry to separate cellulose fibers by removing lignin. In this process, the lignin chips are dissolved in a water solution alkalized to pH 13 with NaOH and heated to around 170 °C, partially hydrolyzing the lignin bonds. The lignin is then precipitated using Na_2S, which replaces some hydroxyl groups with –SH groups, covalently bonding sulfur to the lignin. Annually, about 50–70 million tons of lignin are produced through this method. However, most of this lignin is burned as a low-value fuel to generate electricity and heat in paper mills and bioethanol distilleries.[17]

Lignosulfonate lignin is extracted by adding SO_2 to an alkaline aqueous solution, resulting in sulfonation of the lignin and formation of a precipitate. Soda lignin, obtained using a soda solution, has a high pH and temperature during extraction, with carbonate used to precipitate the lignin. Soda lignin, free from sulfur, has more active sites for chemical modification compared to kraft lignin.[18] Organosolv lignin is derived from the organosolv pulping process, which uses a mixture of water and organic solvents with an acid (mineral or organic) to break covalent bonds between lignin and the hemicellulose matrix at temperatures between 150 and 200 °C. This process yields high-purity lignin, although the associated solvents can be toxic and difficult to separate from the final product.

Lignin's molecular weight ranges between 1000 and 20 000 g mol^{-1}, with its degree of polymerization difficult to predict due to degradation during extraction.[19] The glass transition temperature (T_g) of lignin varies with moisture content, molecular weight, extraction method, cross-link density, and measurement method, typically falling between 70 and 170 °C.[20] Decomposition temperature also varies based on lignin source, extraction method, and measurement techniques, [21] with distinct decomposition observed between 360 and 480 °C *via* thermogravimetry.[22] Lignin exhibits strong UV-vis light absorption due to its high concentration of unsaturated groups and conjugated structures. These properties also enable lignin to demonstrate other optical phenomena, such as light emission and fluorescence. Its optical properties vary depending on the extraction method, resulting in a diverse range of structural compositions.[23] Lignin's mechanical properties are influenced by various factors, including temperature, humidity, chemical exposure, molecular weight, degree of polymerization, and its specific chemical structure. For instance, lignin's Young's modulus ranges from 2.5 to 3.7 GPa at 12% moisture content,[24,25] while its tensile strength spans from 25 to 75 MPa.[26,27] Although lignin is typically associated with rigidity, it can enhance the flexibility and stretchability of materials when combined with other polymers. This counterintuitive behaviour can be attributed to lignin's ability to act as a plasticizer, disrupting the orderly packing of polymer chains and increasing material flexibility. Additionally, lignin may form numerous specific secondary interactions with polymers, which can further improve flexibility and enable effective energy dissipation during stretching, making the resulting material more adaptable and resilient under mechanical stress.[28] Lignin exhibits peculiar electrical properties. Chupka *et al.* demonstrated that lignins have a work function in the conductivity range of 2.0 to 2.2 eV, positioning them as promising candidates for dielectric and semiconducting applications. The electrical behavior of lignin is highly influenced by its functional groups, such as carboxyl, carbonyl, quinoid, and phenolics, which contribute to its electronic and ionic components. Lignin's conductivity is further enhanced by carbocations at phase separations, which activate conductive mechanisms. Furthermore, as an amorphous heterogeneous polymer, lignin's electrophysical properties are highly tunable, depending on its chemical composition, isolation method, and the experimental conditions during preparation.[29–31]

Lignin valorization in organic electronics and bioelectronics

Lignin-based flexible electronics

The unique combination of mechanical and optical properties of lignin[12] makes it an appealing candidate for biodegradable components in flexible electronic devices.

Flexible electronics demand components that can withstand bending, stretching, and twisting without compromising performance. Traditionally, these components, including substrates, electrodes, and active layers, are made from materials like plastic films, metal foils, and flexible glass. While these materials offer some flexibility, their reliance on non-renewable petroleum resources and the prevailing linear "take, make, and dispose" production model pose significant sustainability challenges. As the global demand for electronics surges by 4.52% annually, there is the need for a shift towards circular and eco-friendly solutions.[32] Materials science and engineering advancements have boosted the development of wood-based flexible electronics, which offers the potential for full recyclability and reuse.[33,34]

Q. Fu *et al.*[35] developed a novel approach to create a flexible electronic substrate from wood. The process involves two key steps: (1) removal of lignin and hemicellulose from the wood, to synthesize a transparent cellulose-based structure, which was

then pressed and dried to form a robust substrate, and (2) converting the extracted lignin into conductive carbon fibers (LCFs) through a process developed by Graichen *et al.*[36] These LCFs are then incorporated into the cellulose film using a rod coating technique, forming conductive patterns that can be further defined using a laser printer, as shown in Fig. 2a and b. This method is based on the fundamental principle that the mechanical properties of woody materials depend on the inter- and intramolecular interactions between lignin and cellulose,[37] and effectively repurposed lignin into a functional component of the electronic circuit, demonstrating a circular economy approach to material utilization.

The LCF-printed transparent wood film has demonstrated effective performance in powering LED circuits (Fig. 2c and d).

Edberg *et al.* developed a novel thick-film paper supercapacitor incorporating cellulose nanofibrils (CNF), the mixed ion-electron conducting polymer PEDOT (poly(3,4-ethylenedioxythiophene): polystyrene sulfonate), and sulfonated lignin (LS).[38]

Microstructural analysis using advanced techniques such as atomic force microscopy (AFM), X-ray photoelectron spectroscopy (XPS), and grazing-incidence wide-angle X-ray scattering (GIWAXS), revealed[39] that in the absence of LS, PEDOT : PSS forms a conductive cladding layer around the cellulose fibrils. This configuration not only enabled high electronic and ionic conductivity but also provided good stability, allowing the supercapacitor to scale its performance effectively with increasing thickness. The incorporation of LS, a redox-active organic material,[38] into this system significantly improved the charge storage capacity of the paper supercapacitor. LS leverages its phenolic groups to store electrical energy by cycling between benzoquinone and hydroquinone forms when a positive potential is applied, making it an effective positive electrode material in supercapacitors and batteries. The conductive composite resulted in a notable increase in the specific capacitance from 110 to 230 F g^{-1} and the areal capacitance from 160 mF cm^{-2} to 1 F cm^{-2}. Furthermore, the integration of LS into the electrolyte solution established a stable equilibrium between the electrode and electrolyte, enabling the supercapacitor to endure over 700 charge/discharge cycles without performance degradation. This advancement underscores the potential of lignin-based materials in enhancing the performance and longevity of supercapacitors, positioning them as a viable option for high-capacity, flexible energy storage solutions.

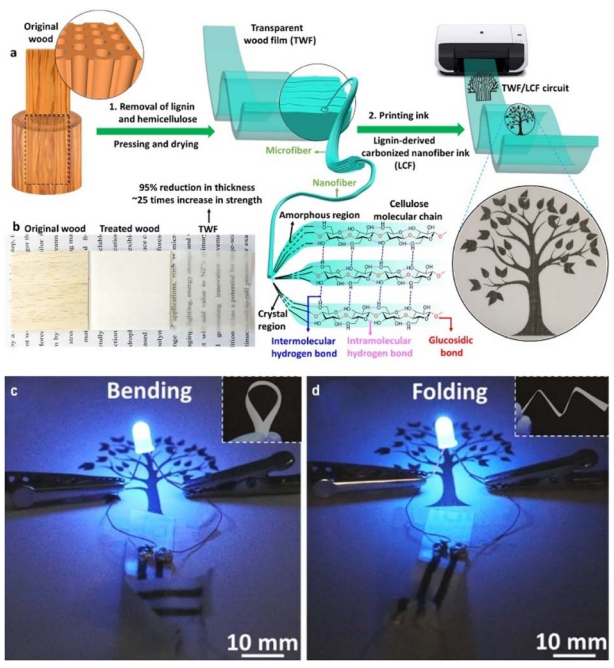

Fig. 2 Transparent wood film processing. Lignin and hemicellulose were removed, and the treated sample was dried and pressed under ambient conditions and then the LCF ink was printed on the substrate (a). Original wood-treated wood and transparent wood film (b). LFC-printed circuit boards connected to a battery powered LED (c and d). Reproduced with permission from Fu *et al.* (2020).[35] Copyright 2020, American Chemical Society.

As a natural biopolymer with multiple hydrophilic or hydrophobic functional groups, lignin is a good candidate for gel electrolyte fabrication in the production of batteries. One effective method for transforming lignin into a gel is through physical cross-linking, which requires specific solvents based on the type of lignin used. Gong *et al.* pioneered the synthesis of a lignin-based gel electrolyte (GE) using a solution casting method with lignin gran fibers as the raw material.[40] They began by dissolving commercial gran lignin fibers in water to create a slurry, which was then heated to 60 °C for 6 hours on a glass plate to form a dry membrane. This membrane was subsequently immersed in a mixture of ethylene carbonate, dimethyl carbonate, and ethyl methyl carbonate (EC/DMC/EMC) to enhance the gel's ionic conductivity. The resulting gel exhibited a capacity in the Li//GE//LiFePO4 full battery approaching its theoretical value of 129 mA h g^{-1} at 1.5C. The authors noted that reducing the size of lignin fibers improved liquid uptake and, consequently, the conduction efficiency of the gel. This method has become a foundational approach in the development of lignin-based ionic-conductive gels.[10]

Building on this work, Song *et al.*[41] applied the solution casting method to produce gel electrolytes from commercial lignocellulose (LC) for Li–S batteries. They categorized LC fibers into five length ranges and found that shorter fibers generally resulted in lower ionic conductivity. Among the various fiber lengths, those in the 150–300 μm range (designated as G2) demonstrated superior mechanical integrity, lithium transference efficiency, and thermal stability. When used in a Li–S full battery, the G2 gel electrolyte facilitated the formation of a stable passivation layer on the electrode surface and hydrogen bonds between polysulfides and the LC matrix. This resulted in a specific capacity of 304.4 mA h g^{-1} at 80 mA g^{-1} after 100 cycles, compared to only 15.5 mA h g^{-1} for a Li//liquid electrolyte//S battery due to active material loss. The porosity of the gel electrolyte significantly influenced its liquid absorption capability, impacting overall performance.

Qiu *et al.*[42] expanded these studies by subjecting the LC membrane to an additional freeze-drying step after casting, to get a lignocellulosic neutral hydrogel (LC-FD) and, consequently, an LC-FD-Li_2SO_4 electrolyte for supercapacitors. The

freeze-drying process significantly increased the porosity and surface area of the hydrogel, which in turn improved its ionic conductivity. Consequently, the LC-FD demonstrated superior liquid absorption capability, as shown in Fig. 3a–d (upper panel).

The freeze-drying process was also found to stabilize water molecules within the hydrogel by enabling stronger interactions between the water and the oxygen-containing functional groups in the LC-FD film (Fig. 3, lower panel).

The assembled supercapacitor with LC-FD-Li_2SO_4 gel electrolyte demonstrated excellent performance, operating effectively at 1.8 V. It provided an energy density of 16.08 W h kg^{-1} and a power density of 225.25 W kg^{-1}, significantly surpassing the maximum energy density of liquid electrolyte-based supercapacitors.

In addition to physical crosslinking, another method to convert lignin-based materials into gel electrolytes involves chemical crosslinking. This approach uses a grafting method to chemically bond different main chains, creating a covalently crosslinked gel electrolyte. Polymers like PEG and its derivatives, such as PEGDGE, are commonly employed in these grafting reactions with the lignin skeleton. A significant challenge in this process is effectively connecting the bulk lignin to the polymer chains. [10] To address this, Liu and his team[43] pre-functionalized PEG and lignin by converting the hydroxyl groups of lignin to alkene and introducing thiol groups to PEG through esterification. This pre-functionalization is crucial for activating the chemical sites needed for the photo-redox thiolene reaction, which links the two polymers. The resulting lignin-*graft*-PEG 2000 product, a dark brown slurry solid, demonstrated modest ionic conductivity when mixed with lithium bis(trifluoromethanesulfonimide) (LiTFSI), making it a potential candidate for solid electrolyte applications. While this specific electrolyte has not yet been utilized in a complete battery assembly, it represents a promising avenue for developing new polymer electrolytes through grafting and copolymerization of lignin. Building on this significant finding, other researchers have explored simplified methods for cross-linking reactions between polymer chains and bulk lignin. Beyond supercapacitors, lignin/PEGDGE electrolytes are being considered for various energy storage devices.[10]

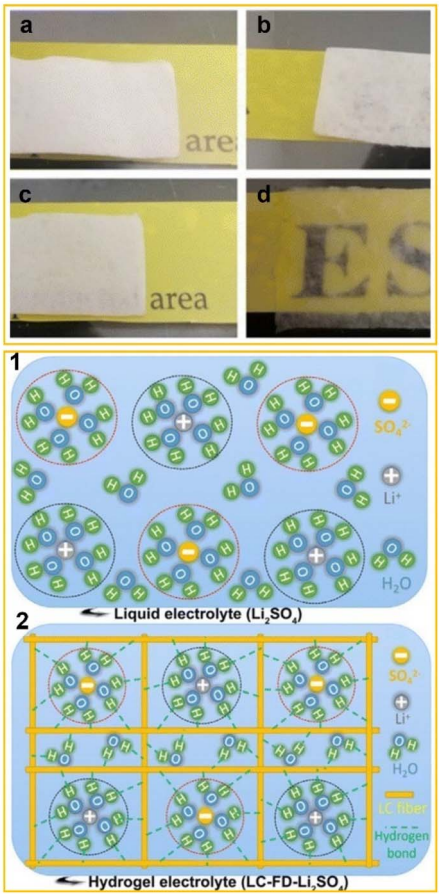

Fig. 3 Upper panel: optical image of an LC membrane (a), LC-FD membrane (b), LC membrane-based hydrogel electrolyte LC-Li_2SO_4 (c) and LC-FD membrane-based hydrogel electrolyte LC-FD-Li_2SO_4 (d). Lower panel: schematic diagram of the liquid electrolyte (1) and hydrogel electrolyte (2). Adapted from Qiu *et al.* (2020).[42] Copyright 2020, Elsevier Ltd.

For example, de Haro *et al.*[44] explored the use of these materials in aqueous dye-sensitized solar cells (DSSCs, *vide infra*).

Lignin derivatives, as insulating materials, are also being introduced into printed circuit boards (PCBs). Many researchers have investigated the use of lignin derivatives in epoxy-based insulating materials for PCBs. Despite achieving good results in product performance, the high preparation costs made lignin derivatives less competitive compared to petroleum-based equivalents. To address this, Komiya *et al.*[45] focused on using soda lignin in epoxy-based insulating materials for PCBs. Though soda lignin is a by-product of the paper industry, and, therefore, is advantageous in terms of production volume and cost (*vide supra*), one of the drawbacks of using it is that it contains cellulose and SiO_2, and the lignin itself is polydisperse, presenting challenges in achieving uniform quality and performance. To mitigate these issues, Komiya's research aimed to develop an innovative epoxy-based bioplastic utilizing the functionality of soda lignin. Epoxy resins are important thermosetting polymers known for their high strength, good dielectric behavior, and resistance to chemicals and corrosion. These properties can be further enhanced by modifying them with hardening agents or fillers, making them suitable for various applications, including electronic devices.[46] In Komiya's study, epoxy resins were cured with soda-lignin (SLG), isolated from black liquor recovered from the soda pulping process, and with methanol-extracted SLG (me-SLG). For the methanol extraction, 100 g of SLG was poured into 1000 cm^3 of methanol. The resulting casting systems, DGEBA/SLG and DGEBA/me-SLG, demonstrated promising structural properties for use in PCBs. Structure images of the materials are shown in Fig. 4.

Since methanol-extracted soda lignin (me-SLG) is processed into a low-molecular-weight compound, its hydroxyl groups exhibit greater chemical reactivity than those in native lignin and soda lignin (SLG). This increased reactivity indicates successful cleavage of ether bonds between the phenylpropane

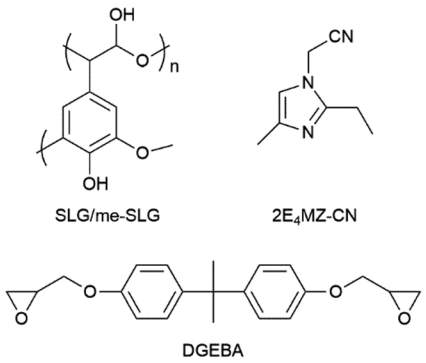

Fig. 4 Chemical structures of SLG/me-SLG, 2E4Mz-CN, and diglycidyl ether of bisphenol-A (DGEBA). Reproduced from G. Komiya *et al.* (2013).[45] Copyright 2013, IEEE.

units, which are lignin monomers, and other units in the complex macromolecule. Consequently, the reactivity with DGEBA (diglycidyl ether of bisphenol A) was improved, resulting in DGEBA/me-SLG having a higher glass transition temperature (T_g). Additionally, DGEBA/me-SLG demonstrated greater flexural strength and lower viscosity compared to DGEBA/SLG, indicating that me-SLG functioned effectively as a phenolic hardener in the DGEBA/me-SLG casting system. The decrease in flexural strength observed in the DGEBA/SLG system was attributed to the presence of SiO_2. The methanol extraction process not only reduced the molecular weight of lignin but also removed SiO_2. Given that herbaceous biomass and SLG contain polydisperse lignin and ash, including SiO_2, this simple process enables the production of low-cost lignin. G. Komiya *et al.* aimed to fabricate an aluminum-based printed circuit board using epoxy resin cured with me-SLG. They incorporated 80 wt% Al_2O_3 into DGEBA/me-SLG and conducted a trial manufacture of an aluminum-based printed circuit board. The resulting board met internal standard values for peel strength (above 1.5 N cm^{-1}), dielectric withstanding voltage (above 2.0 kV), and solder dip resistance (over 260 °C for 20 s × 5 cycles). This demonstrated that the aluminum-based printed circuit board made from a DGEBA/me-SLG insulating material, filled with 80 wt% Al_2O_3, achieved standard performance metrics.

Modulating the lignin content in the PCB substrate allows for the creation of devices with varying degrees of rigidity, suitable for flexible electronics. Research by Kari *et al.* [47] demonstrated that polylactic acid (PLA), a thermoplastic polyester derived from renewable resources, can be mixed with lignin to produce a substrate for multilayer printed circuit boards. The substrate material was produced by mixing PLA with Kraft lignin at temperatures ranging from 170 °C to 200 °C, above the melting temperature of PLA but below the degradation temperature of lignin. This temperature range provided optimal viscosity for the PLA-lignin mixture, accommodating lignin contents from 0 to 40 vol%. The mixing was performed in an extruder. The authors chose Kraft lignin due to its near-neutral pH, which ensures a smooth mixture with PLA and avoids damage to the extruder. Additionally, Kraft lignin is readily available and cost-effective. The resulting substrate material can be molded, injection molded, or extruded. Tensile yield stress and tensile elongation (at yield) were measured for the PLA-lignin substrate material. Table 1 presents these results, including the calculated elastic modulus, which assumes the material is linear up to the yield point. The data showed that increasing lignin content decreases the strength of the substrate and increases the elastic modulus. Therefore, reducing lignin content enhances flexibility, beneficial for non-rigid circuits, while higher lignin content is suitable for rigid circuit boards. The dielectric properties, including relative permittivity (ε_r) and the loss factor (tan δ), were measured at low (1 MHz) and high (1 GHz) frequencies, as shown in Table 1.

From the Table, it is evident that increasing the lignin content raises both the relative permittivity and the loss factor at low and high frequencies. Despite this, the dielectric properties of PLA do not appear to be significantly affected by the addition of lignin, indicating that the composite retains its functionality. Therefore, a lignin-PLA composite can serve as an effective substrate material for circuit boards, similar to pure PLA. Given that lignin is considerably cheaper than PLA, the lignin-PLA composite offers a cost-effective alternative for biodegradable circuit boards. Moreover, this composite allows for modulating the stiffness of the substrate, making it suitable for both rigid and flexible electronics. These advantages could drive the development of innovative biodegradable electronic devices, catering to the expanding flexible electronics market.

Kraft lignin can also be utilized as a gate dielectric material for Organic Field-Effect Transistor (OFET) devices. In a recent study by D'Orsi *et al.*, [48] they investigated the application of two types of kraft lignin, named L1 and L2, derived from softwood through the kraft process. They performed extensive characterization of these lignins using techniques such as Fourier transform infrared spectroscopy, gel permeation chromatography, and nuclear magnetic resonance spectroscopy to understand

Table 1 Mechanical and dielectric properties of the PLA-lignin substrate as a function of lignin content[47]

Lignin content, p	Tensile elongation (%)	Tensile yield stress (MPa)	Elastic modulus (Mpa)	ε_r, 1 MHz	tan δ, 1 MHz	ε_r, 1 GHz	tan δ, 1 GHz
0%	2.6	60	2300	4.6	0.008	3.1	0.003
10%	1.8	48	2700	4.6	0.009	3.3	0.005
20%	1	32	3200	4.9	0.011	3.4	0.008
30%	—	—	—	5.1	0.013	3.6	0.011
40%	—	—	—	5.3	0.015	3.7	0.013

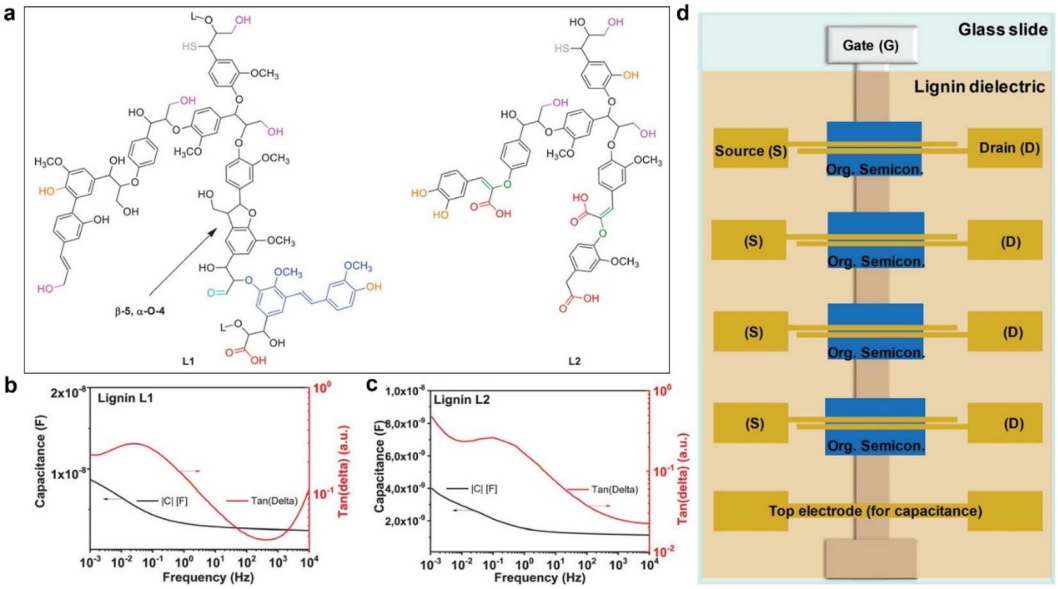

Fig. 5 Schematic representation of L1 and L2 chemical structures, with the indication of the most commonly occurring chemical functionalities (a). (b and c) Dielectric spectroscopy in a frequency range from 10 kHz to 1 mHz of (b) L1 and (c) L2 lignin. Schematic of the mask design for transistor fabrication (d): the gate electrode (G) was aluminum, while the source (S) and drain (D) electrodes were gold for pentacene semiconductors and aluminum for fullerene C60-based OFETs. Reproduced from R. D'Orsi *et al.* (2022).[48] Copyright 2022, Wiley-VCH GmbH.

their chemical structures and degrees of molecular degradation. The schematic representations of L1 and L2 chemical structures provided by the authors (Fig. 5a) reveal that L2 contains more enol ethers (green) and carboxylic groups (red).

To evaluate the potential of L1 and L2 lignin as gate materials for organic field-effect transistors (OFETs), dielectric spectroscopy analyses were performed using a metal–insulator–metal (MIM) structure. In this setup, layers of L1 and L2 lignin were placed between 1 mm wide, 80 nm thick aluminum electrodes arranged in a cross geometry. The dielectric spectroscopy data (Fig. 8) reveals that L1 lignin exhibits significantly more uniform dielectric behavior compared to L2. L1 maintains a relatively constant capacitance across the entire frequency range and demonstrates low dielectric losses, with a maximum loss value of 0.25 even at 1 MHz (indicated by the red line in Fig. 5c. Additionally, the loss angle curve for L1 shows relaxation within a frequency window that is not significant for the fast electrical measurements required in OFETs (evidenced by the dome shape of the red curve in Fig. 5c. Both L1 and L2 lignin were used to fabricate OFETs in a staggered bottom-gate top-contact geometry. The details of this fabrication process are extensively covered in the original papers by D'Orsi *et al.* [48–50] Fig. 5d illustrates the schematic of the OFET layers and geometry used in these devices. They explored two dielectric configurations: an inorganic–organic bilayer of alumina and lignin, and a stand-alone lignin dielectric. OFETs with L1 showed significantly better performance, with higher field-effect mobility and lower hysteresis compared to L2. This is attributed to the higher purity and better interface properties of L1, which also has a lower inorganic ash content compared to L2.[51] Devices using L1 as a stand-alone dielectric performed well, particularly with C60 as the semiconductor layer. However, when interfaced with pentacene, only L1 provided convincing results. The superior performance of L1 is likely due to its ability to facilitate better self-organization of the semiconductor on its surface, enhancing the charge carrier mobility. To sum up, L1 lignin demonstrated the best performance as a gate dielectric for OFET devices, with lower hysteresis and higher charge carrier mobilities. This makes it a promising candidate for future developments in solution-processable electronic devices, potentially enabling low-cost fabrication routes for electronics.

Lignin in bioelectronics

Lignin as a biocompatible material. Lignin generally exhibits good biocompatibility (*vide supra*), an essential property for materials intended for use in biological systems. However, assessing lignin's cytotoxicity can be challenging due to variations in lignin type and extraction methods, which significantly affect its molecular composition and, consequently, its biocompatibility. Therefore, specific cytotoxicity evaluations are necessary for each lignin variant. Lignin's potential as a biomaterial is enhanced by its inherent properties. Its molecular structure includes phenolic and oxygen-containing groups (*vide supra*) that can scavenge or inhibit free radicals, providing antioxidant benefits. The antioxidant activity of lignin is closely linked to its polyphenolic structure. For instance, research by Wang *et al.* demonstrated that lignin fractions with lower molecular weights and more phenolic groups exhibited higher antioxidant activity.[52]

Azadfar *et al.* further explored lignin's antioxidant properties by analyzing lignin derived from wheat straw pretreated with ozone and aqueous ammonia. They found that this lignin, characterized as *p*-hydroxyphenyl-guaiacyl-syringyl (H-G-S)

lignin, demonstrated excellent antioxidant performance, comparable to commercial antioxidants such as guaiacol and butylated hydroxytoluene. The DPPH assay revealed that pretreated lignin achieved an inhibition percentage of 86.9%, while guaiacol and butylated hydroxytoluene reached higher inhibition percentages of 103.6% and 103.3%, respectively. Further research into maintaining antioxidant properties in lignin-based copolymers could broaden their use in applications requiring antioxidant functionality.[53] In addition to antioxidant properties, lignin also possesses antibacterial properties, attributed to its phenolic compounds, which can damage bacterial cell membranes and cause bacterial lysis. Specifically, lignin's phenolic fragments with double bonds and methyl groups have shown antibacterial activity.[54]

Research by Alzagameem *et al.* indicated that different lignin types exhibit varying levels of antimicrobial activity, with organosolv lignin from softwood showing the highest activity, followed by kraft lignin from softwood and organosolv lignin from grass.[55]

Given its range of beneficial biosafety properties, lignin is actively being investigated for use in medical and bioelectronic devices, including biosensors, hydrogels for electronic skin, and artificial neural networks.

Lignin-based bioelectronic devices. Flexible wearable strain sensors are increasingly used in electronic skin, motion detection, and medical monitoring. These devices convert physical signals into electrical ones to collect and transmit information, mimicking the physiological functions of receptors. Conductive hydrogels have emerged as promising candidates for these applications due to their flexibility, stretchability, high electrical conductivity, and biocompatibility.[56] However, current hydrogels face challenges related to mechanical strength and adhesion. Poor mechanical and adhesive properties compromise signal stability, often requiring additional tape for fixation, which can worsen signal stability. [57] Therefore, research is focused on developing hydrogels with improved mechanical and adhesive properties while maintaining excellent electrical conductivity, UV shielding, and antibacterial functions. To enhance these properties, nanofillers are added to conventional polymeric hydrogel matrices. [58] Nanofillers help maintain the hydrogel's internal network under external stress. Among these, cellulose nanocrystals (CNCs), derived from natural polymers, are becoming popular as reinforcing fillers due to their cost-effectiveness compared to expensive materials like graphene oxide and carbon nanotubes.[59] Despite their excellent mechanical properties, hydrogels with CNCs often experience a decrease in adhesive strength over time, leading to unstable signal transmission. Recent research has shifted towards lignin-based hydrogels, utilizing free radical polymerization. Y. Hao *et al.* have developed a dual-catalytic strategy to coat CNCs with lignosulfonate (Ls). This process, which includes catechol redox with Ag and ammonium persulfate (APS) at ambient temperature, rapidly synthesizes multifunctional CNC@Ls-Ag-PAM nanocomposite hydrogels. In their method, the Ls-Ag redox couple activates APS, which is then combined with acrylamide monomers (AM), CNCs, and *N*,*N*′-methylene bisacrylamide (MBA) to create the nanocomposite hydrogels. The process,

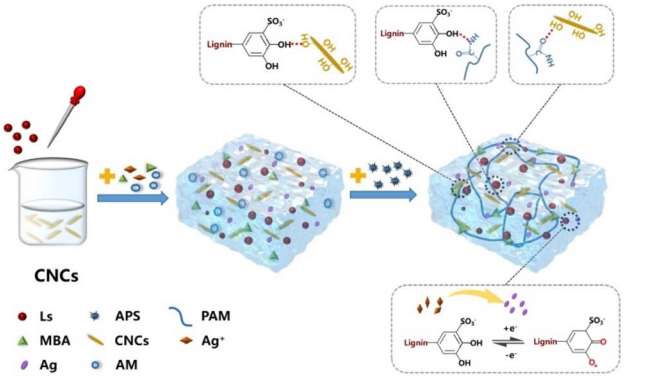

Fig. 6 Schematic illustration of a dynamic redox dual catalytic system based on Ls-Ag and APS for rapid polymerization to form multifunctional hydrogels at room temperature. Reproduced from Y. Hao *et al.* (2022).[61] Copyright 2022, Elsevier Ltd.

shown in Fig. 6, involves Ag^+ converting to Ag nanoparticles (NPs) through electron transfer, while catechol groups in lignin convert to semiquinone/quinone forms. The resulting free electrons from the surface plasmon resonance of Ag NPs facilitate a reversible redox reaction between quinone and catechol groups, ensuring continuous adhesion of the hydrogel.[60]

This hydrogel demonstrated a remarkable combination of toughness, high deformation sensitivity, adhesion, antibacterial properties, and UV protection. The integration of CNCs and Ls into the hydrogel significantly enhanced its tensile strength (406 kPa) and polymerization rate compared to previous hydrogels based on catechol chemistry. CNCs, acting as reinforcing nanofillers, formed multiple hydrogen bonds with Ls-Ag, which substantially improved the hydrogel's toughness.

The CNC@Ls-Ag-PAM hydrogels exhibited exceptional mechanical properties, strong adhesion, high strain sensitivity, fast response times, UV shielding, and antibacterial capabilities. These attributes make them suitable for direct application on human skin to monitor various physiological signals, offering a novel approach for developing epidermal sensors in human–machine interfaces.[61]

Tian *et al.* fabricated a large-scale Electrolyte-Gated Transistor (EGT) array, consisting of 10 × 10 transistors, using a coplanar-gate structure with lignin as the electrolyte.[62] The work of Tian *et al.*[62] addresses a significant gap. Previously, large-scale EGT arrays with inorganic electrolytes existed, and small-scale arrays with organic electrolytes were reported. However, traditional fabrication techniques using bottom or top gate structures were incompatible with organic electrolytes because the acids used in lithography processes would damage these materials. To overcome this issue, Tian *et al.* [62] employed a coplanar gate design developed by Zhu *et al.*, [63] which positions the source, drain, and gate electrodes on the same side of the dielectric layer. This design prevents acid from contacting and damaging the organic electrolyte. Fig. 7a shows a photograph of the large-scale coplanar gate EGT array and a schematic of a single device in the array.

The coplanar-gate IGZO (indium-gallium-zinc-oxide) synaptic transistor array with a lignin electrolyte mimics

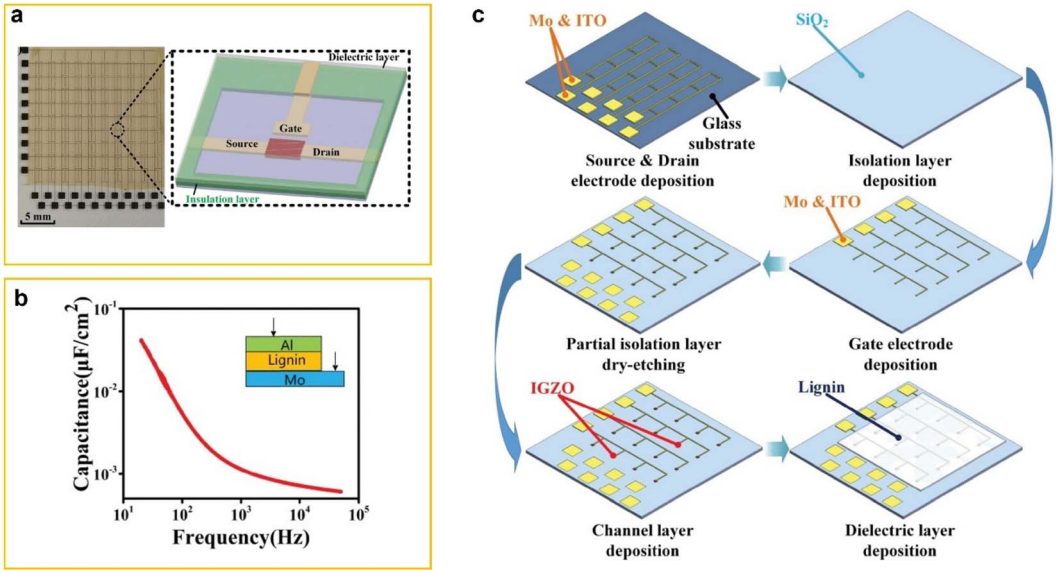

Fig. 7 (a) Schematic images of a real product photograph of a coplanar-gate IGZO (indium-gallium-zinc-oxide) synaptic transistor array with lignin electrolyte (left) and schematic photograph of a single device in the array (right). (b) Frequency-dependent specific capacitance of lignin film. (c) Schematic of the EGT array fabrication process. (1) 150 nm Mo and 50 nm ITO are deposited on a 200 × 200 mm^2 glass substrate by magnetron sputtering. (2) A 300 nm SiO_2 isolation layer is deposited *via* PECVD. (3) 150 nm Mo and 50 nm ITO are deposited, patterned, and wet-etched to form the gate electrode. (4) Partial dry etching of the isolation layer. (5) 60 nm IGZO is deposited. (6) Lignin solution is spin-coated at 500 rpm for 30 s, forming a 380 nm film, and dried for 10 min. Reproduced from X. Tian *et al.* (2022).[63] Copyright 2022, IEE.

biological synaptic behavior. In this setup, the lateral gate electrode functions as the presynapse, receiving input signals, while the IGZO channel acts as the postsynaptic terminal, responsible for outputting the excitatory postsynaptic current (EPSC). Fig. 7b shows the frequency-dependent capacitance of the lignin film, measured using an Al/Lignin/Mo (metal–insulator–metal, MIM) sandwich configuration (inset of Fig. 7). When lignin is dissolved in a binary solvent, its molecules form an electric double layer (EDL) at the Al/electrolyte and Mo/electrolyte interfaces. This EDL results in a specific electrolyte capacitance of 41 nF cm^{-2} at 20 Hz.

Fig. 7c illustrates the detailed fabrication process of the EGT array. This breakthrough is particularly significant for applications in Artificial Neural Networks (ANNs). The EGT array's ability to replicate key synaptic functions, such as EPSC, paired-pulse facilitation (PPF), and high-pass filtering, demonstrates its potential for simulating ANN behavior. These properties are essential for creating complex structures that model the interconnected processing units (neurons) in ANNs, enabling advanced computational tasks.

Following a similar approach, Zhang *et al.*[64] also utilized a photolithographic process to fabricate a 10 × 10 EGT array on glass substrates, employing a polyvinyl alcohol (PVA)/lignin hybrid film as the gate dielectric layer. The vertical sandwich structure used for measuring capacitance, consisting of Mo/lignin and PVA film/Al, is shown in Fig. 8.

In their study, the authors explored the effect of different lignin/PVA mass ratios on the performance of the composite electrolyte films. They found that a mass ratio of 4 : 1 resulted in a higher bilayer capacitance of 740 nF cm^{-2} at a frequency of

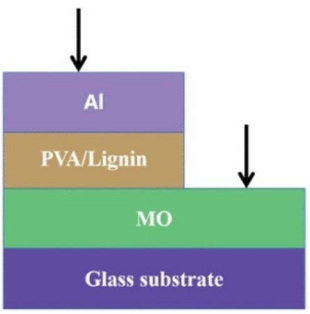

Fig. 8 Vertical sandwich structure of Mo/lignin and PVA film/Al. Adapted from W. Zhang *et al.* (2023).[65] Copyright 2023, IEE.

20 Hz. The array demonstrated successful synaptic properties, including excitatory postsynaptic current (EPSC) and paired-pulse facilitation (PPF). Additionally, with a pulse duration of 100 ms, the energy consumption of the transistor was measured at 0.63 nJ. The artificial synaptic transistor array effectively simulated dynamic memory and forgetting functions, showcasing its potential for advanced applications.

Lignin in organic photovoltaics

Organic photovoltaic technology (OPV) offers a cost-effective, flexible, lightweight, and potentially high-efficiency alternative to inorganic or silicon-based photovoltaics.

Recent advancements in materials synthesis and device design have boosted the power conversion efficiencies (PCEs) of organic solar cells to ~18%. Companies like CSEM/Sunew

Brazil, Epishine Sweden, Kolon Industries Korea, and Moresco Japan are developing and commercializing OPV modules. Recently, the French CEA and Japanese Toyobo announced a 25% efficiency for indoor OPVs.[65]

Fig. 9 shows a schematic device architecture for a typical bulk heterojunction solar cell (BHJ OPV).[2] The photoactive layer is placed between a transparent anode and a low-work-function cathode. The transparent anode typically consists of a thin layer of high-work-function materials like indium tin oxide (ITO), NiO, or MoO_3, deposited on a glass or plastic substrate. The cathode is usually made of aluminum (Al) or calcium (Ca).

To improve the performance and stability of BHJ solar cells, additional interfacial layers are often inserted between the anode and the photoactive layer (Hole Transporting Layers, HTL) and/or between the cathode and the photoactive layer (Electron Transporting Layers, ETL).

Since the early research in organic solar cells, numerous interfacial materials have been developed. Poly(3,4-ethylenedioxythiophene) doped with poly(4-styrene sulfonate) (PEDOT : PSS) has become the most widely used anode interfacial material, serving as the HTL in OPVs.[2] However, PEDOT : PSS has several drawbacks, including: (i) significant electrical and microstructural inhomogeneity, resulting in variable conductivities and morphologies across the film surface, (ii) its acidic nature, which can corrode adjacent layers and hence accelerate device degradation, and (iii) it's hydrophilicity, facilitating device degradation when exposed to environmental moisture.

Lignosulfonates have been introduced as dopants for PEDOT, offering tunable work-functions and conductivities to optimize the anode interface. Li and Hong, [66] drawing inspiration from the electron transfer mechanisms involved in the oxidation of phenol derivatives in lignin, conducted a comprehensive study on sulfomethylated lignin (SL). They evaluated several key properties of SL, including hole mobility, oxidation behavior, electron spin resonance (ESR), and electrochemical characteristics. Their goal was to gain a deeper understanding of SL's performance in hole transport applications. Building on these insights, they developed a novel hole transport material, PEDOT : SL. The authors fabricated polymer solar cells with the device structure ITO/HTM/PTB7/Al, using PEDOT : SL, spin-coated from an aqueous solution, as the HTL. For comparison, they also prepared devices with the same structure but used PEDOT : PSS as the HTL. The hole transport performance of PEDOT : SL was found to be comparable to that of the conventional PEDOT : PSS. Specifically, devices incorporating PEDOT : SL in mass ratios of 1 : 1, 1 : 2, and 1 : 3 achieved PCEs of 5.79%, 5.76%, and 5.33%, respectively. In contrast, devices using PEDOT : PSS typically reported PCEs of 4.28% and 4.50% in the literature.[67,68] This result was surprising because lignosulfonate, which has a complex chemical structure, was expected to offer poorer hole transport properties compared to the more regular structure of PSS. The unexpected high performance of PEDOT : SL was attributed to the efficient electron transfer during the oxidation of electron-rich phenol derivatives and the unique aggregation properties of lignosulfonate.

A high PCE up to 8.47% was achieved in OPV devices by Hong *et al.* with the structure ITO/HTL/PTB7-Th/PFN/Al, using grafted sulfonated-acetone-formaldehyde lignin (GSL) as a dopant to replace PSS as a conducting PEDOT material.[69] For comparison, they also fabricated devices with the same structure using PEDOT : PSS as the HTL, achieving a PCE of 8.39%.

The thermostabilities of PEDOT : GLSs and the stability tests of the devices with PEDOT : GLSs were evaluated. As shown in Fig. 10, at 200 °C the mass residue ratios of PEDOT : PSS and PEDOT : GSLs were all in the range 90–92.5%.

As demonstrated in Fig. 10B, the durability test results of solar cells showed that PEDOT : GSL-1 : 4 had better durability compared to the other PEDOT : GSL samples. However, PEDOT : PSS exhibited superior durability over PEDOT : GSL-1 : 4. After 480 hours, the PCE of the solar cells using PEDOT : GSL-1 : 4 as the HTL was 7.0%, close to the 7.27% PCE of PEDOT : PSS.

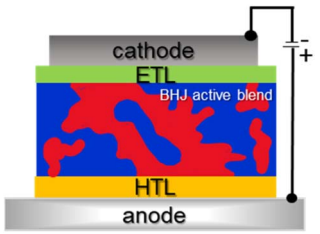

Fig. 9 Schematic representation of a Bulk Heterojunction (BHJ) solar cell.

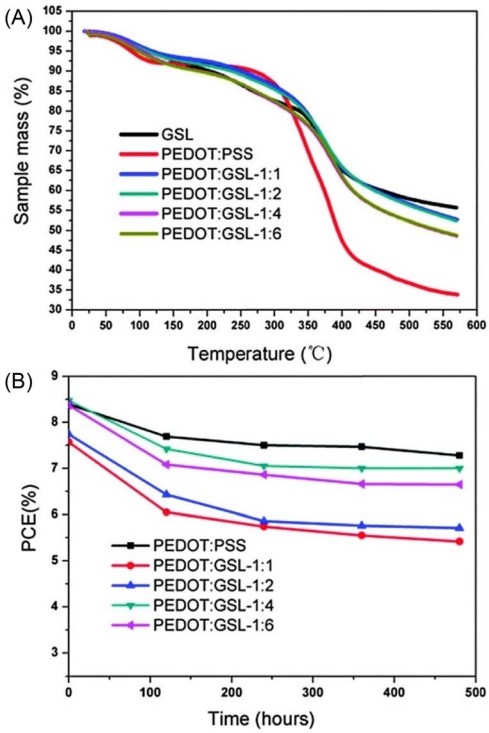

Fig. 10 (A) Thermogravimetric analyses (TGA) of GSL polymer, PEDOT : PSS and PEDOT : GSLs. (B) Lifetime tests of the solar cells based on PEDOT : PSS and PEDOT : GSLs as HTLs, respectively. Reproduced from N. Hong *et al.* (2016).[66] Copyright 2016, Royal Society of Chemistry.

It is worth mentioning that PEDOT : GSL exhibited high performances also in organic light emitting diodes (OLEDs).[69]

Hu *et al.*[70] developed an efficient isotropic ETL by combining demethylsulfated lignin (DMeKL) with perylenediimide (PDIN). This combination significantly enhanced electron transfer and collection, leading to an optimal PCE of 16.0%, surpassing the 15.4% achieved with a pristine PDIN interlayer. Moreover, the interaction between DMeKL and PDIN chemical bonds effectively resolved phase separation issues, further improving the performance and stability of the solar cells.

Very recently, Zhang *et al.*[71] developed a composite from industrial Kraft lignin and bathocuproine to constitute the cathode interface layer (ETL). This combination significantly enhanced the stability of organic solar cells, leveraging electron transfer and hydrogen bonding between the phenol groups in lignin and the phenanthroline in bathocuproine. Introducing lignin served multiple purposes: it spatially blocked substantial contact between bathophenanthroline and non-fullerene materials and chemically attenuated the electron-rich nature of bathophenanthroline. This lignin-based binary interface strategy effectively inhibited unwanted chemical interactions, thereby improving the efficiency and stability of the devices.

Challenges and opportunities of lignin in organic electronics and bioelectronics

Technological and materials challenges

Organic materials often suffer from instability, degrading when exposed to air, water, or light. This presents a significant challenge for both organic electronic and bioelectronic devices. The former must withstand operational environments, while the latter must maintain functionality within living organisms.

Improving the conductivity of organic compounds without compromising their properties is another hurdle. Lignin offers a potential solution due to its abundance and versatility in deriving various organic molecules. However, its complex structure and variable properties, depending on its source and extraction method, hinder its direct application. Additionally, removing impurities from lignin is often complex and costly. To unlock lignin's full potential in electronics, a deeper understanding of its molecular behaviour is essential. Key R&D areas include developing methods to tailor lignin's properties for specific applications, creating new materials with enhanced electrical and mechanical properties, incorporating lignin-based materials into functional electronic devices.

Scalability and cost-effectiveness

To move from laboratory-scale prototypes to commercial products, the production of lignin-based organic electronics must become both scalable and cost-effective. Fortunately, lignin derived from black liquor is abundant and can be extracted using relatively simple processes. Additionally, using printing techniques for device fabrication aligns well with the need for large-scale and low-cost production.

Environmental and sustainability considerations

Organic electronics offer environmental advantages over traditional silicon-based technologies due to their potential for reduced material consumption and waste generation. Lignin-based materials are compatible with printing processes, further enhancing the sustainability profile of these devices. However, end-of-life management and recycling remain crucial challenges. Developing effective recycling methods for lignin-based electronics is essential to minimize environmental impact.

While the paper industry currently utilizes a portion of its lignin for energy generation, transitioning to alternative sustainable energy sources would enable the full allocation of lignin for higher-value applications like electronics.

Conclusions

Lignin offers benefits such as high carbon content, thermal stability, biodegradability, and stiffness, making it a promising biopolymer for supporting a circular economy.

This perspective highlights innovative uses of lignin in organic and bioelectronics. Lignin holds promise for creating transistors and other electronic and bioelectronic devices, offering a sustainable alternative to petroleum-based materials.

It is now clear that during the past decade outstanding results have been achieved in the field of lignin-based electronics and bioelectronics. Several studies have addressed aspects such as enhancing the conductivity of lignin-based films, innovation in fabrication techniques enhancing device performance and stability, and advancing polymerization methods using lignin for advanced materials.

While research into lignin's use in other fields, such as hybrid perovskites,[72–74] dye sensitized solar cells,[75,76] and memory storage devices,[77,78] is outside the scope of this perspective, these efforts illustrate lignin's broad potential across a variety of technologies.

Despite its promise, lignin presents challenges in organic electronic and bioelectronic applications due to its inherent variability in properties, which impacts device performance consistency. Additionally, understanding the mechanisms by which lignin functions within these devices is crucial. Traditional pulping methods may introduce impurities, which complicates its use in advanced applications. Developing scalable production methods and addressing recycling processes are also critical challenges. To overcome these obstacles, further research is needed to refine production techniques, enhance material quality, and evaluate the cost-effectiveness of lignin-based solutions.

Given the pressing need for sustainable materials in organic electronics and bioelectronics, it is worth highlighting lignin's potential in comparison to other renewable resources like cellulose and silk. Cellulose paper, known for its environmental friendliness and biodegradability, faces its own challenges, such as hydrophilicity, which complicates its integration into electronic devices, and the randomly distributed fibers that limit its mechanical strength. Numerous studies have sought to overcome these limitations by enhancing the interfibril

bonding and reducing natural voids through methods such as nanocellulose fabrication, wet stretching, and crosslinking. However, these approaches often involve complex, expensive pretreatments that undermine cellulose's cost-efficiency.[79] Similarly, while silk boasts impressive performance characteristics, [80] its high production costs and susceptibility to supply fluctuations limit its practicality. In contrast, lignin's inherent properties, including its hydrophobicity and mechanical strength, make it more suitable for applications requiring water stability and structural rigidity. As the most abundant aromatic biopolymer in lignocellulosic biomass, lignin is both widely available and affordable to produce *via* established delignification methods. This makes it a more viable material for sustainable electronic and bioelectronic applications.

Ultimately, the combined advantages of lignin's accessibility, structural properties, and environmental sustainability make it a key player in advancing greener technologies. To unlock its full potential, further research is needed to refine its processing, improve material quality, and assess the cost-effectiveness of lignin-based solutions across a broader range of applications. Advances in lignin processing and application could lead to significant improvements in technology and sustainability.

Data availability

No primary research results, software or code have been included and no new data were generated or analysed as part of this perspective.

Author contributions

L. T.: conceptualization, writing – original draft. A. M.: conceptualization, methodology, resources, writing – review & editing, supervision.

Conflicts of interest

There are no conflicts to declare.

References

1 D. Kai, L. P. Chow and X. J. Loh, in *Functional Materials from Lignin: Methods and Advances*, 2018, pp. 1–28, DOI: **10.1142/9781786345219_0001**.
2 A. Marrocchi, *Sustainable Strategies in Organic Electronics*, Elsevier Ltd, Duxford, UK, 2022.
3 M. I. Vladu, E. D. Glowacki, N. S. Sariciftci and S. Bauer, *Green Materials for Electronics*, Wiley-VCH Verlag GmbH & Co. KGaA, 2017.
4 E. Taylor, How Covid, climate change, and Trump created a Global Chip Shortage, **https://www.worldpoliticsreview.com/how-covid-climate-change-and-trump-created-a-global-chip-shortage/**, accessed 06-01, 2023.
5 P. Cosseddu and M. Caironi, *Organic Flexible Electronics: Fundamentals, Devices, and Applications*, 2020.
6 S. Park, M. Takakuwa, K. Fukuda, S. Lee, T. Yokota and T. Someya, *MRS Bull.*, 2023, **48**, 999–1012.
7 H. Malik, M. B. K. Niazi, W. Miran, A. M. Tawfeek, Z. Jahan, E. M. Kamel, N. Ahmed and M. Saeed Akhtar, *Chemosphere*, 2023, **336**, 139213.
8 N. George, A. Adlakha, P. Gupta and A. Debroy, in *Biopolymers for Biomedical Applications*, 2024, pp. 333–372, DOI: **10.1002/9781119865452.ch13**.
9 A. Siddiqa, Z. Yhobu, D. H. Nagaraju, M. Padaki, S. Budagumpi, V. R. Pasupuleti and J.-W. Lim, *Energy Fuels*, 2023, **37**, 2498–2519.
10 X. Yang, Y. Zhang, M. Ye, Y. Tang, Z. Wen, X. Liu and C. C. Li, *Green Chem.*, 2023, **25**, 4154–4179.
11 Y. Tong, J. Yang, J. Li, Z. Cong, L. Wei, M. Liu, S. Zhai, K. Wang and Q. An, *J. Mater. Chem. A*, 2023, **11**, 1061–1082.
12 H. Liu, Y. Guan, L. Yan, Y. Zheng, C. Si and L. Dai, *Green Chem.*, 2024, **26**, 9281–9294.
13 W. Boerjan, J. Ralph and M. Baucher, *Annu. Rev. Plant Biol.*, 2003, **54**, 519–546.
14 D. Kai, M. J. Tan, P. L. Chee, Y. K. Chua, Y. L. Yap and X. J. Loh, *Green Chem.*, 2016, **18**, 1175–1200.
15 J. J. Liao, N. H. A. Latif, D. Trache, N. Brosse and M. H. Hussin, *Int. J. Biol. Macromol.*, 2020, **162**, 985–1024.
16 J. C. del Río, A. Gutiérrez, I. M. Rodríguez, D. Ibarra and Á. T. Martínez, *J. Anal. Appl. Pyrolysis*, 2007, **79**, 39–46.
17 H. Luo and M. M. Abu-Omar, *Green Chem.*, 2018, **20**, 745–753.
18 A. Vishtal and A. Kraslawski, *Bioresearch*, 2011, **6**, 3547–3568.
19 W. O. S. Doherty, P. Mousavioun and C. M. Fellows, *Ind. Crops Prod.*, 2011, **33**, 259–276.
20 B. Wunderlich, D. M. Bodily and M. H. Kaplan, *J. Appl. Phys.*, 2004, **35**, 95–102.
21 O. Faix and D. Meier, *Holz Roh- Werkst.*, 1989, **47**, 67–72.
22 G. Chauvette, M. Heitz, M. Rubio, J. Khorami, E. Chornet and H. Ménard, *Thermochim. Acta*, 1985, **84**, 1–5.
23 H. Liu, Y. Guan, L. Yan, Y. Zheng, C. Si and L. Dai, *Green Chem.*, 2024, **26**, 9281–9294.
24 W. J. Cousins, *Wood Sci. Technol.*, 1976, **10**, 9–17.
25 W. J. Cousins, R. W. Armstrong and W. H. Robinson, *J. Mater. Sci.*, 1975, **10**, 1655–1658.
26 K. Hofstetter, C. Hellmich, J. Eberhardsteiner and H. A. Mang, *Mech. Adv. Mater. Struct.*, 2008, **15**, 474–484.
27 T. K. Bader, K. Hofstetter, C. Hellmich, J. Eberhardsteiner and Z. Angew, *Math. Mech.*, 2010, **90**, 750–767.
28 Q. Wang, J. Guo, X. Lu, X. Ma, S. Cao, X. Pan and Y. Ni, *Int. J. Biol. Macromol.*, 2021, **181**, 45–50.
29 M. Baloch, M. Alberro and J. Labidi, *Polymers*, 2021, **13**, 643.
30 É. I. Chupka and T. M. Rykova, *Chem. Nat. Compd.*, 1983, **19**, 78–80.
31 A. O. Chinomso Iroegbu and S. S. Ray, *ACS Omega*, 2022, **7**, 10854–10863.
32 I. D. Williams and O. S. Shittu, *Detritus*, 2022, **21**, 45–54.
33 X. Wang, T. Xu, M. J. de Andrade, I. Rampalli, D. Cao, M. Haque, S. Roy, R. H. Baughman and H. Lu, The Interfacial Shear Strength of Carbon Nanotube Sheet Modified Carbon Fiber Composites, in *Conference Proceedings of the Society for Experimental Mechanics Series - Challenges in*

Mechanics of Time Dependent Materials, ed. M. Silberstein and A. Amirkhizi, Springer, Cham, 2021, vol. 2.
34 Y. Yazaki, *Nat. Prod. Commun.*, 2015, **10**, 505–512.
35 Q. Fu, Y. Chen and M. Sorieul, *ACS Nano*, 2020, **14**, 3528–3538.
36 F. H. M. Graichen, W. J. Grigsby, S. J. Hill, L. G. Raymond, M. Sanglard, D. A. Smith, G. J. Thorlby, K. M. Torr and J. M. Warnes, *Ind. Crops Prod.*, 2017, **106**, 74–85.
37 L. J. Gibson, *J. R. Soc., Interface*, 2012, **9**, 2749–2766.
38 J. Edberg, O. Inganäs, I. Engquist and M. Berggren, *J. Mater. Chem. A*, 2018, **6**, 145–152.
39 A. Malti, J. Edberg, H. Granberg, Z. U. Khan, J. W. Andreasen, X. Liu, D. Zhao, H. Zhang, Y. Yao, J. W. Brill, I. Engquist, M. Fahlman, L. Wågberg, X. Crispin and M. Berggren, *Advanced Science*, 2016, **3**, 1500305.
40 S.-D. Gong, Y. Huang, H.-J. Cao, Y.-H. Lin, Y. Li, S.-H. Tang, M.-S. Wang and X. Li, *J. Power Sources*, 2016, **307**, 624–633.
41 A. Song, Y. Huang, X. Zhong, H. Cao, B. Liu, Y. Lin, M. Wang and X. Li, *J. Membr. Sci.*, 2018, **556**, 203–213.
42 F. Qiu, Y. Huang, G. He, C. Luo, X. Li, M. Wang and Y. Wu, *Electrochim. Acta*, 2020, **363**, 137241.
43 H. Liu, L. Mulderrig, D. Hallinan, Jr. and H. Chung, *Macromol. Rapid Commun.*, 2021, **42**, e2000428.
44 J. C. de Haro, E. Tatsi, L. Fagiolari, M. Bonomo, C. Barolo, S. Turri, F. Bella and G. Griffini, *ACS Sustain. Chem. Eng.*, 2021, **9**, 8550–8560.
45 G. Komiya, T. Imai, A. Happoya, T. Fukumoto, H. Sagae, N. Sone and A. Takahashi, *IEEE Trans. Compon., Packag., Manuf. Technol.*, 2013, **3**, 1057–1062.
46 T. Imai, F. Sawa, T. Nakano, T. Ozaki, T. Shimizu, M. Kozako and T. Tanaka, *IEEE Trans. Dielectr. Electr. Insul.*, 2006, **13**, 319–326.
47 K. Luukko, H. Kähäri and S. Fors, *PCT Pat.*, WO2013144420A1, 2013.
48 R. D'Orsi, C. V. Irimia, J. J. Lucejko, B. Kahraman, Y. Kanbur, C. Yumusak, M. Bednorz, F. Babudri, M. Irimia-Vladu and A. Operamolla, *Adv. Sustainable Syst.*, 2022, **6**, 2200285.
49 M. Egginger, M. Irimia-Vladu, R. Schwödiauer, A. Tanda, I. Frischauf, S. Bauer and N. S. Sariciftci, *Adv. Mater.*, 2008, **20**, 1018–1022.
50 C. Yumusak, N. S. Sariciftci and M. Irimia-Vladu, *Mater. Chem. Front.*, 2020, **4**, 3678–3689.
51 R. D'Orsi, J. J. Lucejko, F. Babudri and A. Operamolla, *ACS Omega*, 2022, **7**, 25253–25264.
52 G. Wang, Y. Xia, B. Liang, W. Sui and C. Si, *J. Chem. Technol. Biotechnol.*, 2018, **93**, 2977–2987.
53 M. Azadfar, A. H. Gao, M. V. Bule and S. Chen, *Int. J. Biol. Macromol.*, 2015, **75**, 58–66.
54 J. L. Espinoza-Acosta, P. I. Torres-Chávez, B. Ramírez-Wong, C.-M. López-Saiz and B. Montaño-Leyva, *BioResources*, 2016, **11**, 5452–5481.
55 A. Alzagameem, S. E. Klein, M. Bergs, X. T. Do, I. Korte, S. Dohlen, C. Hüwe, J. Kreyenschmidt, B. Kamm, M. Larkins and M. Schulze, *Polymers*, 2019, **11**, 670.
56 S. Xia, Q. Zhang, S. Song, L. Duan and G. Gao, *Chem. Mater.*, 2019, **31**, 9522–9531.
57 C. Dang, M. Wang, J. Yu, Y. Chen, S. Zhou, X. Feng, D. Liu and H. Qi, *Adv. Funct. Mater.*, 2019, **29**, 1902467.
58 Z. Zhao, R. Fang, Q. Rong and M. Liu, *Adv. Mater.*, 2017, **29**, 1703045.
59 H. Liu, T. Xu, C. Cai, K. Liu, W. Liu, M. Zhang, H. Du, C. Si and K. Zhang, *Adv. Funct. Mater.*, 2022, **32**, 2113082.
60 J. Ke, C. Niu, J. Zhang and G. Zeng, *J. Mol. Catal. A: Chem.*, 2014, **395**, 276–282.
61 Y. Hao, C. Wang, W. Jiang, C. G. Yoo, X. Ji, G. Yang, J. Chen and G. Lyu, *Int. J. Biol. Macromol.*, 2022, **221**, 1282–1293.
62 X. Tian, T. Zhao, J. Li, T. Li, L. Yuan, X. Xue, Z. Wang and J. Zhang, *IEEE Trans. Electron Devices*, 2022, **69**, 2325–2330.
63 L. Q. Zhu, C. J. Wan, L. Q. Guo, Y. Shi and Q. Wan, *Nat. Commun.*, 2014, **5**, 3158.
64 W. Zhang, J. Y. Li, L. Cheng, W. Shi, Y. Lei, S. Wen, F. Wang, J. Jiang, P. Wen and J. Zhang, *IEEE Trans. Electron Devices*, 2023, **70**, 3245–3250.
65 C. Rollet, *An organic solar cell with 25% efficiency*, **https://www.pv-magazine.com/2020/03/24/an-organic-solar-cell-with-25-efficiency/**, Last accessed: September 2024.
66 Y. Li and N. Hong, *J. Mater. Chem. A*, 2015, **3**, 21537–21544.
67 M. V. Srinivasan, M. Ito, P. S. Kumar, K. M. Abhirami, N. Tsuda, J. Yamada, P. K. Shin and S. Ochiai, *Ind. Eng. Chem. Res.*, 2015, **54**, 181–187.
68 S. Guo, B. Cao, W. Wang, J.-F. Moulin and P. Müller-Buschbaum, *ACS Appl. Mater. Interfaces*, 2015, **7**, 4641–4649.
69 N. Hong, J. Xiao, Y. Li, Y. Li, Y. Wu, W. Yu, X. Qiu, R. Chen, H.-L. Yip, W. Huang and Y. Cao, *J. Mater. Chem. C*, 2016, **4**, 5297–5306.
70 H.-C. Hu, H. Xu, J. Wu, L. Li, F. Yue, L. Huang, L. Chen, X. Zhang and X. Ouyang, *Adv. Funct. Mater.*, 2020, **30**, 2001494.
71 Q. Zhang, T. Liu, S. Wilken, S. Xiong, H. Zhang, I. Ribca, M. Liao, X. Liu, R. Kroon, S. Fabiano, F. Gao, M. Lawoko, Q. Bao, R. Österbacka, M. Johansson and M. Fahlman, *Adv. Mater.*, 2024, **36**, 2307646.
72 Y. Wu, J. Wang, X. Qiu, R. Yang, H. Lou, X. Bao and Y. Li, *ACS Appl. Mater. Interfaces*, 2016, **8**, 12377–12383.
73 G. A. Al-Dainy, F. Watanabe, G. K. Kannarpady, A. Ghosh, B. Berry, A. S. Biris and S. E. Bourdo, *ACS Omega*, 2020, **5**, 1887–1901.
74 Y. Li, T. Liu, X. Qiu, Y. Zhou and Y. Li, *ACS Sustain. Chem. Eng.*, 2019, **7**, 961–968.
75 X. Wang, H. Guo, Z. Lu, X. Liu, X. Luo, S. Li, S. Liu, J. Li, Y. Wu and Z. Chen, *ACS Appl. Mater. Interfaces*, 2021, **13**, 33536–33545.
76 W. Cheng, C. Wan, X. Li, H. Chai, Z. Yang, S. Wei, J. Su, X. Tang and Y. Wu, *J. Energy Chem.*, 2023, **83**, 549–563.
77 Y. Park and J.-S. Lee, *ACS Appl. Mater. Interfaces*, 2017, **9**, 6207–6212.
78 S. De Stefano, O. Durante, R. D'Orsi, A. Operamolla, M. Ambrico, P. F. Ambrico, N. Martucciello, F. Giubileo and A. Di Bartolomeo, *J. Mater. Chem. C*, 2024, **12**, 13621–13631.
79 B. Jiang, C. Chen, Z. Liang, S. He, Y. Kuang, J. Song, R. Mi, G. Chen, M. Jiao and L. Hu, *Adv. Funct. Mater.*, 2020, **30**, 1906307.
80 M. Irimia-Vladu and N. S. Sariciftci, *Polym. Int.*, 2024, DOI: **10.1002/pi.6697**.